Thermal Shifts of the Spectral Lines in the $^4F_{3/2}$ to $^4I_{11/2}$ Manifold of an Nd:YAG Laser

SHAO ZHONG XING AND J. C. BERGQUIST

Abstract—**We report the thermal shifts of eleven of the twelve lines from the $^4F_{3/2}$ Stark energy levels to the $^4I_{11/2}$ energy levels in an Nd:YAG laser for a temperature change from 20–200°C. The thermal shift difference between the Stark sublevels R_1, R_2 in $^4F_{3/2}$ is found to be about -0.6 ± 0.6 cm^{-1}/100°C. Within our experimental uncertainty, all of the lasing lines either moved to longer wavelength or remained unchanged with increasing temperature.**

Introduction

RECENT advances in high-power diode lasers have led to extremely efficient, CW operation of neodymium-doped crystal and fiber lasers [1]–[3]. There have also been important strides toward low threshold operation of miniature hybrid and monolithic neodymium-doped lasers [1], [4], [5]. These devices have inherently much better mode quality and frequency stability than the diode lasers used as the pump sources. Additionally, several new nonlinear crystals that are used to double these lasers into the visible have been developed with good optical quality and large nonlinear coefficients [6]–[8].

For these reasons, interest in these devices as ultrastable frequency sources near 1 and 0.5 μm is strong. While there are few atomic and molecular transitions near 1 μm with suitably narrow linewidths to which to lock a laser, there are many such transitions in the visible. One very attractive candidate that we are investigating is the $5d^{10}6s$ $^2S_{1/2}$–$5d^9 6s^2$ $^2D_{5/2}$ transition in a single laser-cooled Hg^+ ion near 281 nm (1.126 μm ÷ 4) [9], [10]. This transition has a natural linewidth of about 1.7 Hz [10], [11]. A laser that has been spectrally narrrowed to less than 1 Hz and tuned to this wavelength could be stabilized to this transition to better than 1×10^{-17}. The accuracy of such a frequency standard should also exceed 1×10^{-17} [12].

We have begun to study various neodymium-doped crystals and fibers to determine their suitability as narrow-band radiation sources whose fourth harmonic could be tuned to match the transition frequency in Hg^+. Unfortunately, the neodymium-doped crystal laser and bulk glass lasers are generally not tunable by more than a few wavenumbers at any temperature. But some of the transitions do tune by as much as several wavenumbers per 100°C change in temperature (generally to lower frequencies). In this letter we report on our measurements of the thermal shifts of the spectral lines in the $^4F_{3/2}$ to $^4I_{11/2}$ manifold of a neodymium-doped, yttrium-aluminum-garnet (Nd:YAG) laser. Although the linewidths, spectral lineshapes, and thermal shifts of several lines of Nd:YAG have been studied both theoretically and experimentally [13]–[20] we were able to measure the thermal shifts of all the laser lines in this manifold with the exception of the weak R_2–Y_2 transition near 1.0551 μm. Thereby we were able to do a comprehensive study of the temperature dependence of these lines in the temperature range from 20–200°C.

Manuscript received March 9, 1988; revised April 20, 1988. This work was supported in part by the U.S. Air Force Office of Scientific Research and by the Office of Naval Research.

S. Z. Xing is with the Changchun Institute of Optics and Fine Mechanics, Changchun, China, on leave at the Time and Frequency Division, National Bureau of Standards, Boulder, CO 80303.

J. C. Bergquist is with the Time and Frequency Division, National Bureau of Standards, Boulder, CO 80303.

IEEE Log Number 882227.

Experimental Setup

The experimental setup is shown in Fig. 1. Although we used a ring laser cavity, the oscillation of the laser was bidirectional. The radius of curvature of the concave mirrors M_1 and M_2 was 10 cm, and of M_3, 15 cm. M_4 was flat. To ensure that all the lines from the $^4F_{3/2}$ manifold to the $^4I_{11/2}$ manifold would oscillate, all the mirrors were highly reflecting from 1.0–1.15 μm. The 5 mm diameter by 10 mm long Nd:YAG crystal was cut at Brewster's angle for low loss and ease of cleaning. The crystal was placed in the 80 μm beam waist between mirrors M_2 and M_3. The cavity was adjusted to nearly compensate for the astigmatism introduced by the crystal. The Nd:YAG crystal was end pumped by laser light near 750 nm that was focused through mirror M_3. M_3 was nearly 90 percent transmitting at 750 nm. The pump laser was a ring dye laser pumped by a krypton ion laser. The output radiation from the dye laser could be tuned from 735 to 800 nm with as much as 600 mW of power. The oven for the crystal was made of aluminum and was heated by a 15 W thermal plug-heater. A chromel–alumel thermocouple monitored the temperature of the oven. The birefringent filter (BF) consisted of a single quartz plate approximately 5 mm thick. The monochromator is a 0.8 m focal length scanning monochromator with a 150 lines/mm grating blazed for an 8 μm wavelength. A 40 μm slit was generally used in the entrance plane of the monochromator. In the exit plane of the monochromator, a diode array with a resolution of 25 μm was used to receive and display the spectrum signal on an oscilloscope.

Experimental Results

The twelve possible transitions from the upper $^4F_{3/2}$ manifold to the lower $^4I_{11/2}$ manifold in Nd:YAG are

0018-9197/88/0900-1829$01.00

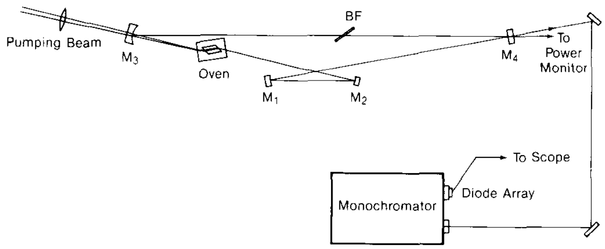

Fig. 1. The setup used to measure the thermal shifts of spectral lines in Nd : YAG laser. The ring laser consists of mirror, M_1, M_2, M_3, and M_4, a single plate birefringent filter (BF), and an Nd : YAG crystal. The Nd : YAG crystal is housed in an oven that can be heated from room temperature to ≥200°C. The crystal is axially pumped by up to 600 mW of power from a ring dye laser tunable near 750 nm. A diode array in the exit plane of the 0.8 m focal length monochromator receives and displays the signal on a scope.

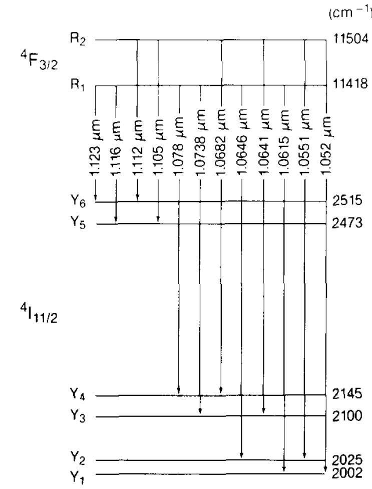

Fig. 2. A simplified optical energy level diagram showing the $^4F_{3/2}$ manifold and the $^4I_{11/2}$ manifold in Nd : YAG. The twelve possible infrared transitions from the upper two Stark sublevels (R_1, R_2) to the lower six Stark sublevels ($Y_1 \rightarrow Y_6$) are also indicated.

shown in Fig. 2. Customarily, the Stark sublevels are labeled with increasing energy as R_1 and R_2 in the $^4F_{3/2}$ manifold and as Y_1 and Y_6 in the $^4I_{11/2}$ manifold. The ring laser oscillated on all of the transitions with the exception of the R_2-Y_2 transition near 1.0551 μm. Some of the light from the Nd : YAG laser that escaped through M_4 was directed into the monochromator. The diode array in the exit plane of the monochromator made it possible to monitor the thermal shift and gain width of each transition easily. The array had 512 diodes and a resolution of 25 μm. To make a thermal shift measurement, the monochromator setting was adjusted until the signal was centered on the diode array. This setting was noted and the birefringent filter was then adjusted to allow another transition to oscillate. By tuning the birefringent filter over the line to find the maximum power, we could roughly determine line center. The monochromator setting was changed to bring the diffracted signal for the wavelength of this transition to the center of the diode array and this setting was noted. Several readings for all eleven transitions were taken at one temperature, then the oven temperature was changed, and the entire process repeated. On most lines, the line center could be measured to only a few tenths of a wavenumber. This limitation was not due to poor signal-to-noise ratio but rather due to large asymmetries in the line. Some of these asymmetries were caused by fundamental asymmetric-broadening mechanisms in the crystal [13]. But the more difficult problem, because of our inability to properly characterize it, was the fact that the different transitions competed to oscillate. Before fully tuning across any line, the laser was likely to jump to another transition. The wavelength at which the jump occurred depended on the birefringent filter position, the mirror reflectances and losses at the various wavelengths, and the gain profile of the different transitions. Because of this systematic uncertainty, the line centers could not be located to better than ± 0.5 cm^{-1}.

In Fig. 3 the thermal shifts of the eleven transitions that lased are plotted as a function of temperature from 20 to 200°C (solid lines). For all lines except the R_1-Y_4 transition at 1.0779 μm and the $R_2 \rightarrow Y_4$ transition at 1.0682 μm, the shifts appear to vary linearly with temperature. The strongly nonlinear thermal movement of these two lines is due to the shift and broadening with temperature of the Y_4 Stark sublevel. In Table I we list the thermal shifts of all the transitions giving an endpoint-to-endpoint average shift for the R_1, $R_2 \rightarrow Y_4$ transitions. From our work there is fivefold redundancy in determining the relative thermal shift of the R_1 and R_2 levels (in principle, there would be sixfold redundancy but this is reduced by 1 since the $R_2 \rightarrow Y_2$ line did not oscillate). While our results are not inconsistent with a zero relative tempera-

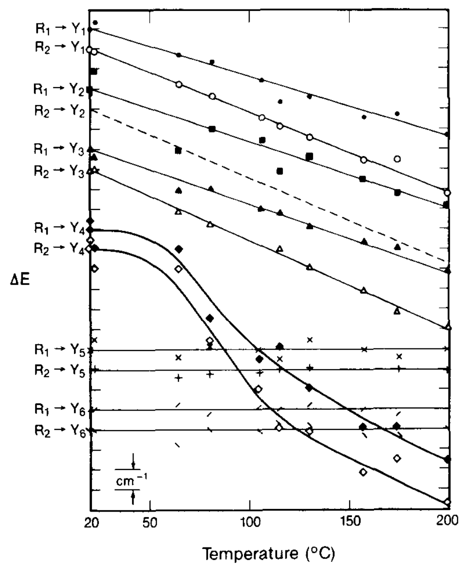

Fig. 3. Plot showing the variation in the wavelength for maximum laser power as a function of Nd : YAG crystal temperature for all 12 lines from the $^4F_{3/2}$ manifold to the $^4I_{11/2}$ manifold. The dotted line is the deduced temperature variation for the $R_2 \rightarrow Y_2$ transition at 1.0551 μm that did not oscillate.

TABLE I
THERMAL SHIFTS OF THE TRANSITIONS BETWEEN THE STARK ENERGY SUBLEVELS IN THE $^4F_{3/2}$ MANIFOLD AND IN THE $^4I_{11/2}$ MANIFOLD, AND THE RELATIVE THERMAL SHIFT OF THE R_1 AND R_2 STARK LEVELS SHIFT IN AN Nd:YAG LASER

			$^4I_{11/2}$					
			Y_1	Y_2	Y_3	Y_4	Y_5	Y_6
$^4F_{3/2}$	R_1	Wavelength(μm)	1.0615	1.0646	1.0738	1.0779	1.1161	1.1225
		Thermal shift (cm^{-1}/100°C)	-3.0	-3.3	-3.5	-6.1	0.0	0.0
	R_2	Wavelength(μm)	1.052	1.0551	1.0641	1.0682	1.1055	1.1121
		Thermal shift (cm^{-1}/100°C)	-4.0	(-4.3)	-4.6	-7.0	0.0	0.0
Relative thermal shift between R_1 & R_2 (cm^{-1}/100°C)			-1.0	(-1.0)	-1.1	-0.9	0.0	0.0

ture shift between R_1 and R_2, there is an indication of a small linear separation of these levels with increasing temperature. This possibility was also noted in [3]. There is twofold redundancy in determining the relative thermal shift of any pair of Stark sublevels in the lower $^4I_{11/2}$ level. These redundancies provide a self-consistency check of the relative movement of the Stark sublevels in each manifold. Thus, we are able to predict the thermal shift of the weak $R_2 \rightarrow Y_2$ 1.0551 μm transition to be approximately -4.3 $cm^{-1}/100°C$. This is plotted as the dashed line in Fig. 2.

Fig. 3 shows that for those lines with shorter wavelength (and stronger intensity), the 1.052, 1.0615, 1.0641, and 1.0738 μm lines, the thermal shifts are roughly linear and the shift difference in each pair is consistent. The 1.052 μm line moves about -7.3 cm^{-1} from room temperature to 200°C or about -4.0 $cm^{-1}/100°C$. This is in agreement with the shift measured by Kushida [13]. The 1.0615 μm line moves about -3.0 cm^{-1} for a temperature change of 100°C. This compares to the -2.7 $cm^{-1}/100°C$ thermal variation measured by Marling [14] and to the -3.8 $cm^{-1}/100°C$ temperature shift measured by Kushida [13]. Thus the relative shift with temperatures of the R_1 and R_2 Stark levels is about -1 $cm^{-1}/100°C$ from this pair of transitions. Almost the same relative thermal shift is obtained for the pair consisting of the 1.0641 μm line (R_2-Y_3) and the 1.0738 μm line (R_1-Y_3). The 1.0641 μm transition moves about -4.6 $cm^{-1}/100°C$ and the 1.0738 μm transition moves about -3.5 $cm^{-1}/100°C$. Thus, this pair indicates a relative shift of about -1.1 $cm^{-1}/100°C$ between the R_1 and R_2 Stark levels.

From these two pairs of lines, it would appear that the R_2 sublevel in the $^4F_{3/2}$ manifold moves to a lower energy with increasing temperature about 1 $cm^{-1}/100°C$ faster than the R_1 level. However, for the lines at 1.1055 μm (R_2-Y_5), 1.1121 μm (R_2-Y_6), 1.1161 μm (R_1-Y_5) and 1.1225 μm (R_1-Y_6) we measured almost no shift for a change of nearly 200°C in temperature. Thus, these lines indicate that R_1 and R_2 shift with temperature at nearly the same rate.

The thermal shift of the 1.0682 μm line (R_2-Y_4) and of the 1.0779 μm line (R_1-Y_4) are strongly nonlinear in this temperature range. Thus it is difficult to determine the relative shift of R_1 and R_2 from this pair. As stated earlier, we did assign an endpoint-to-endpoint average shift for these two lines. This result and the thermal shifts for the remaining transitions are summarized in the table. By assigning equal weight to each of the measured shift differences, we could average our results to give a relative thermal shift of -0.6 ± 0.6 $cm^{-1}/100°C$ between Stark sublevels R_1 and R_2. The error of ± 0.6 $cm^{-1}/100°C$ includes both the statistical and the systematic uncertainties.

DISCUSSION

There are a number of reasons the various transitions in the $^4F_{3/2} \rightarrow {}^4I_{11/2}$ manifold have different measured thermal shifts. The crystalline field at the site of the impurity Nd ion is a function of the local strain. When this strain is dynamically produced by the lattice vibrations, the interaction between the Nd ion and the local crystalline field causes temperature-dependent broadenings and shifts of the energy levels of the ion. The thermal behaviors of linewidths and line positions are frequently dominated by this dynamic phonon–impurity interaction not only in the Nd:YAG crystal but in other impurity:crystalline hosts as well [13]. The crystalline field strength can also be changed by thermal expansion of the crystalline lattice, but this appears to be a minor contribution to the thermal shifts and broadenings in hard crystals such as Nd:YAG [13]. When the temperature of the crystal is increased, energy levels and hence, spectral lines, broaden as the higher phonon states are occupied. Usually, the phonon-impurity interaction lowers an energy level and usually the dependence with temperature of higher levels is larger than for lower levels because of smaller energy denominators. As a result, the spectral lines are generally expected to move to the longer wavelengths when the temperature is increased [13]. This general feature is confirmed by our experimental results.

We also observed that the longer the wavelength the wider the linewidth and the more complex the thermal shift. The shorter wavelength lines have relatively narrow and symmetrical lineprofiles ($\Delta\nu \sim 5$ cm^{-1}) that broaden only slightly with temperature. Therefore we can deduce that both of the upper Stark levels R_2 and R_1 and the lower Stark levels Y_1, Y_2, Y_3 remain spectrally narrow in the temperature range from 20–200°C. We also found the shift of these transitions to be simply linear in this temperature range. The intermediate-wavelength transitions have a wider and asymmetric line profile ($\Delta\nu \gtrsim 10$ cm^{-1}), and from the arguments above, that implies that the Y_4 Stark level is $\gtrsim 5$ cm^{-1} wider than Y_1, Y_2, and Y_3. The fact that the transitions that terminate on the Y_4 Stark level move in a nonlinear fashion with temperature in our measurement range might be explained by the asymmetrical thermal broadening of the Y_4 level. While some of the thermal broadening mechanisms give rise to a symmetrical line shape, other mechanisms, such as the direct, single-resonant-phonon interaction, cause asymmetric broadening [13]. If the line profile, first broadened asymmetrically to the red ($\sim 80°C$) because of the thermal behavior of the Y_4 level, then the measured line shift would appear to move strongly toward the red. If later ($\sim 150°C$) the broadening becomes more symmetric (or asymmetric to the blue) then the rate of the red shift would decrease.

The longest wavelength transitions have the widest linewidths ($\Delta\nu \gtrsim 13$ cm^{-1}) among all the transitions between the $^4F_{3/2}$ and $^4I_{11/2}$ manifolds. Thus the Y_5 and Y_6 Stark sublevels are the broadest in the $^4I_{11/2}$ manifold. Hence the thermal shifts of these transitions are somewhat obscured by the thermal broadening over our relatively small change in temperature. Clearly these upper energy levels in the lower Stark manifold generally move with R_1 and R_2 with change in temperature. These results are in basic agreement with earlier work on the thermal shift of some of these transitions [13]–[18].

Acknowledgment

The authors wish to thank D. Nabors, R. Byer, and T. Baer for many helpful discussions.

References

[1] B. Zhou, T. J. Kane, G. J. Dixon, and R. L. Byer, "Efficient, frequency-stable laser-diode-pumped Nd:YAG laser," *Opt. Lett.*, vol. 10, pp. 62–64, Feb. 1985.

[2] T. M. Baer, "Frequency doubled, diode pumped Nd:YAG laser," *Proc. Soc. Photo-Opt. Instrum. Eng.*, vol. 610, pp. 45–47, Jan. 1986.

[3] R. J. Mears, L. Reekie, S. B. Poole, and D. N. Payne, "Neodymium-doped silica single-mode fibre lasers," *Electron. Lett.*, vol. 21, pp. 738–740, Aug. 15, 1985; I. P. Alcock, A. I. Ferguson, D. C. Hanna, and A. C. Tropper, "Tunable, continuous-wave neodymium-doped monomode-fiber laser operating at 0.900–0.945 and 1.070–1.135 μm," *Opt. Lett.*, vol. 11, pp. 709–711, Nov. 1986.

[4] T. J. Kane and R. L. Byer, "Monolithic, unidirectional single-mode Nd:YAG ring laser," *Opt. Lett.*, vol. 10, pp. 65–67, Jan. 1985.

[5] W. R. Trutna, Jr., D. K. Donald, and M. Nazarathy, "Unidirectional diode-laser-pumped Nd:YAG ring laser with a small magnetic field," *Opt. Lett.*, vol. 12, pp. 248–250, Apr. 1987.

[6] W. J. Kozlovsky, C. D. Nabors, and R. L. Byer, "Efficient second harmonic generation of a diode-laser-pumped CW Nd:YAG laser using monolithic MgO:$LiNbO_3$ external resonant cavities," *IEEE J. Quantum Electron.*, vol. 24, pp. 913–919, June 1988; R. L. Byer "Diode pumped solid state laser," *Science*, to be published; T. Y. Fan, G. J. Dixon, and R. L. Byer, "Efficient GaAlAs diode-laser-pumped operation of Nd:YLF at 1.047 μm with intracavity doubling to 523.6 nm," *Opt. Lett.*, vol. 11, pp. 204–206, Apr. 1986.

[7] See, for example, J. T. Lin and C. Chen, "Choosing a nonlinear crystal," *Laser Optron.*, vol. 6, pp. 59-63, Nov. 1987, and references therein.

[8] T. Baer, "Large-amplitude fluctuations due to longitudinal mode coupling in diode-pumped intracavity-doubled Nd:YAG lasers," *J. Opt. Soc. Amer. B*, vol. 3, pp. 1175–1180, Jan. 1986.

[9] J. C. Bergquist, W. M. Itano, and D. J. Wineland, "Recoilless optical absorption and Doppler sidebands in a single trapped ion," *Phys. Rev. A*, vol. 36, pp. 428–430, July 1, 1987.

[10] J. C. Bergquist, D. J. Wineland, W. M. Itano, H. Hemmati, H.-U. Daniel, and G. Leuchs, "Energy and radiative lifetime of the $5d^96s^2$ $^2D_{5/2}$ state in HgII by Doppler-free two-photon laser spectroscopy," *Phys. Rev. Lett.*, vol. 55, pp. 1567–1570, Oct. 7, 1985.

[11] W. M. Itano, J. C. Bergquist, R. G. Hulet, and D. J. Wineland, "Radiative decay rates in Hg+ from observations of quantum jumps in a single ion," *Phys. Rev. Lett.*, vol. 59, pp. 2732–2734, Dec. 14, 1987.

[12] D. J. Wineland, W. M. Itano, J. C. Bergquist and R. G. Hulet, "Laser cooling limits and single-ion spectroscopy," *Phys. Rev. A*, vol. 36, pp. 2220–2232, Sept. 1, 1987.

[13] T. Kushida, "Linewidths and thermal shifts of spectral lines in neodymium-doped yttrium aluminum garnet and calcium fluorophospate," *Phys. Rev.*, vol. 185, pp. 500–508, Sept. 10, 1969.

[14] J. Marling, "1.05–1.44 μm tunability and performance of the CW Nd^{3+}:YAG laser," *IEEE J. Quantum Electron.*, vol. QE-14, pp. 56–62, Jan. 1978.

[15] A. A. Kaminskii, "High-temperature spectroscopic investigation of stimulated emission from lasers based on crystals and glasses activated with Nd^{3+} ions," *Sov. Phys. JETP*, vol. 27, pp. 388–399, Sept. 1968.

[16] D. E. McCumber and M. D. Sturge, "Linewidths and temperature shift of the *R* lines in ruby," *J. Appl. Phys.*, vol. 34, pp. 1682–1684, June 1963.

[17] W. M. Yen, W. C. Scott, and A. L. Schawlow, "Phonon-induced relaxation in excited optical states of trivalent praseodymium in LaF_3," *Phys. Rev.*, vol. 136, pp. A271–A283, Oct. 5, 1964.

[18] T. Kushida and M. Kikuchi, "*R*, *R'* and *B* absorption linewidths and phonon-induced relaxations in ruby," *J. Phys. Soc. Japan*, vol. 23, pp. 1333–1348, Dec. 1967.

[19] M. Birnbaum and C. F. Klein, "Stimulated emission cross section at 1.061 μm in Nd:YAG," *J. Appl. Phys.*, vol. 44, pp. 2928–2930, June 1973.

[20] V. A. Buchenkov, I. B. Vitrishchak, V. G. Evdokimova, L. N. Soms, A. Stepanov, and V. K. Stupnikov, "Temperature dependence of giant pulse amplification in YAG:Nd^{3+}," *Sov. J. Quantum Electron.*, vol. 11, pp. 702–705, June 1981.